Inorg. Chem. **2002**, *41*, 3820–3829

Ligand Substitution, pH Dependent Deoxygenation, and Linkage Isomerization Reactions of the 2,2′-Bipyridinetetranitroruthenate Dianion

Daniel A. Freedman,*,† Daron E. Janzen,‡ Jennifer L. Vreeland,† Hannah M. Tully,† and Kent R. Mann*,‡

Contribution from the Department of Chemistry, State University of New York at New Paltz, New Paltz, New York 12561, and Department of Chemistry, University of Minnesota, Minneapolis, Minnesota 55455

Received January 29, 2002

The reaction of the $[Ru(bpy)(NO_2)_4]^{2-}$ (bpy = 2,2′-bipyridine) ion in aqueous solutions produces two different nitrosyl complexes, depending on the pH of the solution. At acidic pH, complex *cis,cis*-$Ru(bpy)(NO_2)_2(ONO)(NO)$ was isolated. At neutral or basic pH, $[Ru(bpy)(NO_2)_4]^{2-}$ reacts to give *cis,trans*-$Ru(bpy)(NO_2)_2(NO)(OH)$. Both new complexes were fully characterized by elemental analysis and UV–vis, IR, ^1H NMR, and ^{15}N NMR spectroscopy. A single-crystal X-ray structure of *cis,trans*-$Ru(bpy)(NO_2)_2(NO)(OH)$ was also obtained. *cis,cis*-$Ru(bpy)(NO_2)_2(ONO)(NO)$ isomerizes in acetone or water solution to give a mixture of the *trans,cis*-$Ru(bpy)(NO_2)_2(ONO)(NO)$ and *cis,cis*-$Ru(bpy)(ONO)_2(NO_2)(NO)$ linkage isomers as determined by ^1H and ^{15}N NMR spectroscopy. A single-crystal X-ray structure of a solid solution of *cis,cis*-$Ru(bpy)(ONO)_2(NO_2)(NO)$/*trans,cis*-$Ru(bpy)(NO_2)_2(ONO)(NO)$ was also obtained. This pair of isomers is the first crystallographically characterized compound with nitro, nitrito, and nitrosyl ligands. The kinetic studies of the $Ru–NO_2 \rightarrow Ru–NO$ conversion reactions of $[Ru(bpy)(NO_2)_4]^{2-}$ in buffered solutions from pH 3 to pH 9 complement previous studies of the reverse reaction. The reactions are first order in $[Ru(bpy)(NO_2)_4]^{2-}$. At high pH, the reaction is independent of the concentration of H^+ while, at low pH, the reaction is first order in the concentration of H^+. The rate determining step of the high pH reaction involves breakage of the $Ru–NO_2$ bond while, at low pH, the mechanism involves a rapid reversible protonation of a NO_2 ligand followed by the rate determining loss of hydroxide to produce a nitrosyl ligand.

Introduction

We recently reported the first preparation of the $[Ru(bpy)(NO_2)_4]^{2-}$ anion via the thermal displacement of benzene from $[(\eta^6\text{-Bz})Ru(bpy)Cl]Cl$ (Bz = benzene; bpy = 2,2′-bipyridine) in methanol solution (reaction 1).[1]

$$[(\eta^6\text{-Bz})Ru(bpy)Cl]Cl \xrightarrow[CH_3OH]{\text{xs } KNO_2} K_2[Ru(bpy)(NO_2)_4] + Bz + 2KCl \quad (1)$$

Our original interest in this complex stemmed from investigations of the solvatochromism[2,3] of the analogous $[Ru(bpy)(CN)_4]^{2-}$ anion and their relationship to the development of environmental sensing devices.[4] Like $[Ru(bpy)(CN)_4]^{2-}$, $[Ru(bpy)(NO_2)_4]^{2-}$ is stable in the solid state, but in aqueous solution, $[Ru(bpy)(NO_2)_4]^{2-}$ undergoes reactions we identify here to give nitrosyl complexes. Previously studied ruthenium−nitro compounds are known to reversibly react in protic solvents via oxide transfer to yield ruthenium−nitrosyl complexes (reaction 2).[5−12] This reaction has received increased attention recently because it provides a convenient

* To whom correspondence should be addressed. E-mail: mann@chem.umn.edu (K.R.M.); freedmad@matrix.newpaltz.edu (D.A.F.).
† State University of New York at New Paltz.
‡ University of Minnesota.

(1) Freedman, D. A.; Janzen, D. E.; Mann, K. R. *Inorg. Chem.* **2001**, *40*, 6009.
(2) Bignozzi, C. A.; Chiorboli, C.; Indelli, M. T.; Scandola, M. A.; Varani, G.; Scandola, F. *J. Am. Chem. Soc.* **1986**, *108*, 7872.
(3) Timpson, C. J.; Bignozzi, C. A.; Sullivan, B. P.; Kober, E. M.; Meyer, T. J. *J. Phys. Chem.* **1996**, *100*, 2915.
(4) Evju, J. K.; Mann, K. R. *Chem Mater.* **1999**, *11*, 1425.
(5) Bignozzi, C. A.; Chiorboli, C.; Murtaza, A.; Jones, W. E.; Meyer, T. J. *Inorg. Chem.* **1993**, *32*, 1036.
(6) Godwin, J. B.; Meyer, T. J. *Inorg. Chem.* **1971**, *10*, 471.
(7) Godwin, J. D.; Meyer, T. J. *Inorg. Chem.* **1971**, *10*, 2150.
(8) Borges, S. da S. S.; Davanzo, C. U.; Castellano, E. E.; Z-Schpector, J.; Silva, S. C.; Franco, D. W. *Inorg. Chem.* **1998**, *37*, 2670.
(9) Gomes, M. G.; Sebastiao, S. C.; Lopes, L. G. F.; Santos, P. S.; Franco, D. *J. Chem. Soc., Dalton Trans.* **1998**, 601.
(10) Chen, Y.; Lin, F.-T.; Shepherd, R. E. *Inorg. Chem.* **1999**, *38*, 973.
(11) Nagao, H.; Mukaida, M.; Shimizu, K.; Howell, F. S.; Kakihana, H. *Inorg. Chem.* **1986**, *25*, 4312.

10.1021/ic0255205 CCC: $22.00
Published on Web 06/26/2002

synthetic route to ruthenium−nitrosyl complexes that are of considerable interest for their potential uses as NO scavengers or donors for therapeutic applications.[13−21]

$$L_5Ru(II)-NO_2^{n+} + 2H^+ \rightleftharpoons L_5Ru(II)-NO^{(n+2)+} + H_2O \quad (2)$$

In this report, we describe the synthesis, characterization by ^{15}N NMR, and single-crystal X-ray structure determinations of two different nitrosyl containing products obtained at different pH values from aqueous solutions of $[Ru(bpy)(NO_2)_4]^{2-}$. Kinetic measurements reveal two different pathways for the reaction of $[Ru(bpy)(NO_2)_4]^{2-}$ to form new nitrosyl complexes.

Experimental Section

General Considerations. KNO_2, 2,2′-bipyridine, and HEPES ((4-(2-hydroxyethyl)-1-piperizineethane-sulfonic acid, sodium salt) were purchased from Aldrich. $K^{15}NO_2$ was purchased from Cambridge Isotope Laboratories. $RuCl_3 \cdot xH_2O$ was purchased from Alfa or Aldrich. Combustion analyses were performed by QTI Analytical Laboratories. ^1H NMR spectra were recorded on a JEOL 300 MHz Eclipse or Varian VI-500 MHz spectrometer. ^1H NMR chemical shifts are relative to $(CH_3)_4Si$. ^{15}N NMR spectra were recorded at 30.45 MHz on a JEOL Eclipse spectrometer with a 5 mm probe or at 50.67 MHz on a Varian spectrometer with a 10 mm probe. ^{15}N NMR chemical shifts are relative to ^{15}N-formamide (external reference). A 120 s or 5 s relaxation time was used in the acquisition of the ^{15}N NMR spectra. All ^{15}N NMR spectra were acquired with ^{15}N labeled compounds. UV−vis spectra were recorded on a Ocean Optics Chem-2000 or Perkin-Elmer Lambda-6 spectrometer. IR spectra were recorded on a Perkin-Elmer 1600 FTIR or Nicolet Magna 560 FTIR spectrometer using a multiple internal reflectance accessory.

Preparation of *cis,trans*-Ru(bpy)$(NO_2)_2$(NO)(OH) (1). $K_2[Ru(bpy)(NO_2)_4]$ (0.110 g, 0.212 mmol) was dissolved in 3 mL of 0.10 M, pH 7 HEPES buffer. The solution was stirred at room temperature for 5 days. Over this time, a light yellow precipitate formed. The product was filtered, washed with cold water, and dried in vacuo. The product was isolated as a light yellow powder (0.060 g, 71% yield). Anal. Calcd for $C_{10}H_9N_5O_6Ru$: C, 30.31; H, 2.29; N, 17.67. Found: C, 30.08; H, 2.36; N, 17.38. ^1H NMR (300 MHz, D_2O vs DSS), δ: 8.64 ($H^{6,6'}$, d of d of d, 2H, $J_1 = 8.6$ Hz, $J_2 = 1.4$ Hz, $J_3 = 0.7$ Hz); 8.60 ($H^{3,3'}$, d, 2H, $J = 8.3$ Hz); 8.41 ($H^{4,4'}$, d of t, 2H, $J_1 = 7.9$ Hz, $J_2 = 1.5$ Hz); 7.83 ($H^{5,5'}$, d of d of d, 2H, $J_1 = 7.6$ Hz, $J_2 = 5.7$ Hz, $J_3 = 1.4$ Hz). IR (ATR, cm^{-1}): $\nu_{OH} = 3495$; $\nu_{NO} = 1852$; ν_{as} $(NO_2) = 1416$; $\nu_{sym}(NO_2) = 1329, 1309$; $\delta_{ONO} = 821, 815$.

Preparation of *cis,cis*-Ru(bpy)$(NO_2)_2$(ONO)(NO) (2A). $K_2[Ru(bpy)(NO_2)_4]$ (0.100 g, 0.193 mmol) was dissolved in 5 mL of water. Addition of 0.47 g of a 60% aqueous solution of HPF_6 produced an immediate precipitate. The reaction was stirred for 15 min. The product was filtered and washed with a small amount of cold water and air-dried yielding 0.0639 g (78% yield) of a peach colored powder. Anal. Calcd for $C_{10}H_8N_6O_7Ru$: C, 28.26; H, 1.90; N, 19.76. Found: C, 28.40; H, 1.84; N, 19.76. ^1H NMR (300 MHz, d_6-acetone), δ: 9.86 (H^6, d of d of d, 2H, $J_1 = 5.78$ Hz, $J_2 = 1.65$ Hz, $J_3 = 0.55$ Hz); 9.01 ($H^{6'}$, d of d of d, 2H, $J_1 = 5.64$ Hz, $J_2 = 1.35$ Hz, $J_3 = 0.54$ Hz); 8.89 (H^3, d, 2H, $J = 8.25$ Hz); 8.83 ($H^{3'}$, d, 2H $J = 7.98$ Hz); 8.70 (H^4, t of d, 2H, $J_1 = 7.71$ Hz, $J_2 = 1.38$); 8.45 ($H^{4'}$, t of d, 2H, $J_1 = 7.90$ Hz, $J_2 = 1.38$); 8.24 (H^5, d of d of d, 2H, $J_1 = 6.81$ Hz, $J_2 = 5.92$ Hz, $J_3 = 1.38$ Hz); 7.89 ($H^{5'}$, d of d of d, 2H, $J_1 = 7.71$ Hz, $J_2 = 5.71$ Hz, $J_3 = 1.38$ Hz). IR (ATR, cm^{-1}): $\nu_{NO} = 1914$; ν_{as} $(NO_2) = 1416$; ν_{sym} $(NO_2) = 1335, 1314$; $\delta_{ONO} = 823, 818$.

Preparation of $K_2[Ru(bpy)(^{15}NO_2)_4]$. This compound was prepared from [BzRu(bpy)Cl]Cl and $K^{15}NO_2$ by the method previously described for the unlabeled compound.[1] ^{15}N NMR (30.45 MHz, 85% H_2O/D_2O pH 8), δ: 406, 409 ($^{15}NO_2$).

Preparation of *cis,trans*-Ru(bpy)$(^{15}NO_2)_2(^{15}NO)$(OH) (^{15}N-1). This compound was prepared from $K_2[Ru(bpy)(^{15}NO_2)_4]$ in the same manner as described for *cis,trans*-Ru(bpy)$(NO_2)_2$(NO)(OH). ^{15}N NMR (50.67 MHz, D_2O), δ: 352 ($^{15}NO_2$), 225 (^{15}NO).

Preparation of *cis,cis*-Ru (bpy)$(^{15}NO_2)_2(O^{15}NO)(^{15}NO)$ (^{15}N-2A). This compound was prepared from $K_2[Ru(bpy)(^{15}NO_2)_4]$ in the same manner as described for *cis,cis*-Ru(bpy)$(NO_2)_2$(ONO)(NO). ^{15}N NMR (50.67 MHz, d_6-acetone), δ: 466 ($O^{15}NO$), 338, 336 ($^{15}NO_2$), 257 (^{15}NO).

Isomerization Reaction of 2A to 2B/2C. A solution of **2A** in d_6-acetone was allowed to react at room temperature for 4 days. The resulting solution exhibited the following ^1H NMR (300 MHz) peaks assigned to **2B**, δ: 9.97 (H^6, d of d of d, 2H, $J_1 = 5.76$ Hz, $J_2 = 1.53$ Hz, $J_3 = 0.69$ Hz); 9.07 ($H^{6'}$, d of d of d, 2H, $J_1 = 5.70$ Hz, $J_2 = 1.38$ Hz, $J_3 = 0.64$ Hz); 8.90 (H^3, d, 2H, $J = 7.98$ Hz); 8.83 ($H^{3'}$, d, 2H $J = 7.77$ Hz); 8.73 (H^4, t of d, 2H, $J_1 = 7.71$ Hz, $J_2 = 1.65$); 8.43 ($H^{4'}$, t of d, 2H, $J_1 = 7.83$ Hz, $J_2 = 1.38$); 8.31 (H^5, d of d of d, 2H, $J_1 = 7.70$ Hz, $J_2 = 5.63$ Hz, $J_3 = 1.31$ Hz); 7.94 ($H^{5'}$, d of d of d, 2H, $J_1 = 7.68$ Hz, $J_2 = 5.57$ Hz, $J_3 = 1.38$ Hz). The following peaks in the spectrum were assigned to **2C**, δ: 9.91 (H^6, d of d of d, 2H, $J_1 = 5.91$ Hz, $J_2 = 1.58$ Hz, $J_3 = 0.62$ Hz); 9.24 ($H^{6'}$, d of d of d, 2H, $J_1 = 5.49$ Hz, $J_2 = 1.65$ Hz, $J_3 = 0.62$ Hz); 8.54 ($H^{4'}$, t of d, 2H, $J_1 = 7.80$ Hz, $J_2 = 1.38$); 8.27 (H^5, d of d of d, 2H, $J_1 = 7.68$ Hz, $J_2 = 5.76$ Hz, $J_3 = 1.38$ Hz); 8.07 ($H^{5'}$, d of d of d, 2H, $J_1 = 7.70$ Hz, $J_2 = 5.76$ Hz, $J_3 = 1.38$ Hz). The peaks for H^3, $H^{3'}$, and H^4 are obscured by peaks for **2B**. Integrations of the signals assigned to **2B** and **2C** indicate they are present in a 4.6:1 ratio, respectively. A bulk sample of this mixture for ^{15}N NMR analysis was prepared by refluxing 50 mg of **^{15}N-2A** overnight in dichloromethane and evaporating the solvent to recover the product. A ^1H NMR spectrum of this bulk product was identical to that obtained from the NMR scale reaction in d_6-acetone. The ^{15}N NMR spectrum (30.45 MHz, d_6-acetone) exhibited peaks at 469 ($O^{15}NO$), 460 ($O^{15}NO$), 337($^{15}NO_2$), and 266 (^{15}NO) ppm assigned to **2B** and peaks at 458 ($O^{15}NO$), 344 ($^{15}NO_2$), and 260 (^{15}NO) ppm assigned to **2C**.

Measurement of Kinetic Parameters. Reactions of $K_2[Ru(bpy)(NO_2)_4]$ at different pH values were followed by UV−vis spectroscopy. Buffers (0.10 M) were prepared from boric acid (pH = 8.98), HEPES (pH = 7.0), acetic acid (pH = 5.00, 4.00), and

(12) Ooyama, D.; Miura, Y.; Kanazawa, Y.; Howell, F. S.; Nagao, No.; Mukaida, M.; Nagao, H.; Tanaka, K. *Inorg. Chim. Acta* **1995**, *237*, 47.
(13) Ford, P. C.; Bourassa, J.; Miranda, K.; Lee, B.; Lorkovic, I.; Boggs, S.; Kudo, S.; Laverman, L. *Coord. Chem. Rev.* **1998**, *171*, 185.
(14) Lorkovic, I. M.; Miranda, K. M.; Lee, B.; Bernhad, S.; Schooner, J. R.; Ford, P. C. *J. Am. Chem. Soc.* **1998**, *120*, 11674.
(15) Lopes, L. G. F.; Wieraszko, A. E.-S.; Y.; Clarke, M. J. *Inorg. Chim. Acta* **2001**, *312*, 15.
(16) Togniolo, V.; da Silva, R. S.; Tedesco, A. C. *Inorg. Chim. Acta* **2001**, *316*, 7.
(17) Davies, N. A.; Wilson, M. T.; Slade, E.; Frecker, S. P.; Murrer, B. A.; Powell, N. A.; Henderson, G. R. *Chem. Commun.* **1997**, 47.
(18) Lang, D. R.; Davis, J. A.; Lopes, L. G. F.; Ferro, A. A.; Vasconcellos, L. C. G.; Franco, D. W.; Tfouni, E.; Wieraszko, A.; Clarke, M. J. *Inorg. Chem.* **2000**, *39*, 2294.
(19) Fricker, S. P.; Slade, E.; Powell, N. A.; Vaughan, O. J.; Henderson, G. R.; Murrer, B. A.; Megson, I. L.; Bisland, S. K.; Flitney, F. W. *Br. J. Pharmacol.* **1997**, *122*, 1441.
(20) Fricker, S. P. *Platinum Met. Rev.* **1995**, *39*, 150.
(21) Deb, A.; Paul, P. C.; Goswami, S. *J. Chem. Soc., Dalton Trans.* **1988**, 2051.

Table 1. Crystal Data, Data Collection, and Refinement Parameters for *cis,trans*-Ru(bpy)$(NO_2)_2$(NO)(OH) (**1**) and Solid Solution *cis,cis*-Ru(bpy)$(ONO)_2(NO_2)$(NO)/*trans,cis*-Ru(bpy)$(NO_2)_2$(ONO)(NO) (**2B/2C**)

	1	**2B/2C**
formula	$C_{10}H_9N_5O_6Ru$	$C_{10}H_8N_6O_7Ru$
color, habit	yellow, plate	orange, block
size, mm^3	$0.25 \times 0.23 \times 0.08$	$0.03 \times 0.02 \times 0.01$
lattice type	monoclinic	monoclinic
space group	$P2_1/c$	$P2_1/n$
a, Å	6.5607(6)	7.3635(5)
b, Å	14.233(2)	13.2109(9)
c, Å	14.540(2)	14.684(1)
β, deg	102.080(1)	95.169(1)
V, $Å^3$	1327.6(2)	1422.6(2)
Z	4	4
fw, g mol^{-1}	396.29	425.29
D_{calcd}, g cm^{-3}	1.983	1.986
μ, mm^{-1}	1.221	1.154
$F(000)$	784	840
θ range, deg	2.02−27.54	2.08−25.05
index ranges	$-8 \le h \le 8$, $-18 \le k \le 18$, $-14 \le l \le 18$	$-8 \le h \le 8$, $-14 \le k \le 15$, $-15 \le l \le 17$
reflns collected	9774	8180
unique reflns	3041 (R_{int}=0.0402)	2522 (R_{int}=0.0527)
weighting factors,[a] a, b	0.0704, 0	0.0733, 0.7958
max, min transm	1.0000, 0.6686	1.0000, 0.7809
data, restraints, params	3041/0/233	2522/6/227
R1, wR2 ($I > 2\sigma(I)$)	0.0364, 0.0949	0.0466, 0.1143
R1, wR2 (all data)	0.0419, 0.0983	0.0728, 0.1246
GOF (on F^2)	0.998	1.044
largest diff peak, hole, e $Å^{-3}$	1.537, −1.339	1.111, −0.785

[a] $w = [\sigma^2(F_o^2)+(aP)^2+(bP)]^{-1}$, where $P = (F_o^2 + 2F_c^2)/3$.

chloroacetic acid (pH = 2.90, 3.00, 3.28, and 3.51). The appropriate buffer was added to a 1.0 cm path length quartz cell that was placed in a thermostated cell holder (25.0 °C) and allowed to equilibrate. A small amount of K_2[Ru(bpy)$(NO_2)_4$] was added to the cell and mixed thoroughly before data acquisition was initiated (typically 10 s). Absorbance versus time data were preprocessed to give plots of $\ln(A_t - A_\infty)$ versus t that gave straight lines for at least four half-lives. Values of k_{obs} were obtained from the slopes of the $\ln(A_t - A_\infty)$ versus t plots.

X-ray Structure Determinations. Single crystals were attached to glass fibers and mounted on the Siemens SMART[22] system for data collection at 173(2) K with graphite-monochromated Mo Kα radiation (λ = 0.71073 Å). An initial set of cell constants was calculated from reflections harvested from 3 sets of 20 frames oriented such that orthogonal wedges of reciprocal space were surveyed. Orientation matrices were determined from 40 to 58 reflections. Final cell constants were calculated from a minimum set of 2584 strong reflections from the actual data collection. Data were collected via the hemisphere collection method, surveyed to the extent of 1.3 hemispheres and to a resolution of 0.84 Å. Three major swaths of frames with 0.30° steps in ω were collected. The intensity data were corrected for absorption and decay using SADABS.[23] Space groups were determined on the basis of systematic absences and intensity statistics. Direct-methods solutions provided the positions of most non-hydrogen atoms. Several full-matrix least-squares/difference Fourier cycles were performed to locate the remaining non-hydrogen atoms. All calculations were performed using the SHELXTL-V5.0 suite of programs[24] on INDY R4400-SC or Pentium computers. Crystal and X-ray collection and refinement data are summarized in Table 1. Selected bond lengths and angles are given in Table 2.

Table 2. Selected Bond Lengths (Å) and Angles (deg)[a] for *cis,trans*-Ru(bpy)$(NO_2)_2$(NO)(OH) (**1**) and Solid Solution *cis,cis*-Ru(bpy)$(ONO)_2(NO_2)$(NO)/*trans,cis*-Ru(bpy)$(NO_2)_2$(ONO)(NO) (**2B/2C**)

	1	**2B/2C**
Ru(1)−N(1)	2.091(2)	2.085(5)
Ru(1)−N(2)	2.089(2)	2.079(5)
Ru(1)−N(3)	2.081(3)	*c*
Ru(1)−N(4)	2.076(2)	1.775(5)
Ru(1)−N(5)	1.768(3)	2.072(5)
Ru(1)−N(6A)	*c*	1.99(4)[b]
Ru(1)−O(1)	*c*	2.049(5)
Ru(1)−O(6)	1.917(2)	2.084(13)
N(3)−O(1)	1.238(3)	1.285(7)
N(3)−O(2)	1.223(3)	1.224(7)
N(4)−O(3)	1.227(3)	1.112(6)
N(4)−O(4)	1.240(3)	*c*
N(5)−O(4)	*c*	1.261(6)
N(5)−O(5)	1.137(4)	1.228(6)
N(6A)−O(6A)	*c*	1.19(4)[b]
N(6A)−O(7A)	*c*	1.28(6)[b]
N(1)−Ru(1)−N(2)	78.66(10)	77.78(18)
N(1)−Ru(1)−N(3)	172.90(9)	*c*
N(1)−Ru(1)−N(4)	96.91(10)	95.3(2)
N(1)−Ru(1)−N(5)	94.21(10)	93.51(19)
N(1)−Ru(1)−N(6A)	*c*	85.5(12)[b]
N(2)−Ru(1)−N(3)	96.69(10)	*c*
N(2)−Ru(1)−N(4)	172.14(10)	172.5(2)
N(2)−Ru(1)−N(5)	96.54(10)	87.66(19)
N(2)−Ru(1)−N(6A)	*c*	94.8(8)[b]
N(3)−Ru(1)−N(4)	87.07(11)	*c*
N(3)−Ru(1)−N(5)	91.64(11)	*c*
N(4)−Ru(1)−N(5)	90.24(11)	89.9(2)
N(4)−Ru(1)−N(6A)	*c*	87.4(8)[b]
N(5)−Ru(1)−N(6A)	*c*	177.1(8)[b]
N(5)−Ru(1)−O(6)	178.09(10)	167.9(3)
O(1)−Ru(1)−N(1)	*c*	166.92(18)
O(1)−N(3)−O(2)	120.0(3)	116.4(6)
O(3)−N(4)−O(4)	119.9(3)	*c*
O(4)−N(5)−O(5)	*c*	119.2(5)
O(6)−N(6)−O(7)	*c*	115.9(13)
O(6A)−N(6A)−O(7A)	*c*	113(5)[b]
Ru(1)−N(5)−O(5)	174.5(3)	121.3(4)
Ru(1)−N(4)−O(3)	*c*	172.5(5)

[a] Estimated standard deviation in the least significant figure are given in parentheses. [b] Minor nitrito component. [c] Not applicable.

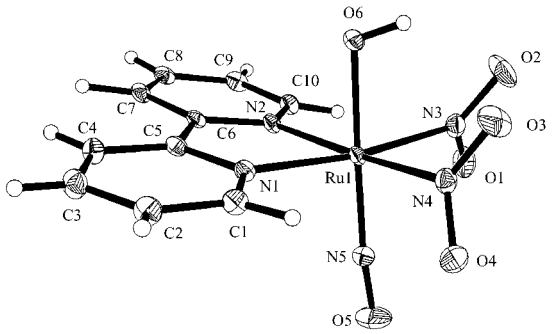

Figure 1. Labeled ORTEP diagram of *cis,trans*-Ru(bpy)$(NO_2)_2$(NO)(OH) (**1**) (30% ellipsoids).

***cis,trans*-Ru(bpy)$(NO_2)_2$(NO)(OH) (1).** A suitable single-crystal grew at room temperature from a solution of K_2[Ru(bpy)$(NO_2)_4$] in a 0.1 M pH 6.4 phosphate buffer (see Scheme 1). An ORTEP diagram of *cis,trans*-Ru(bpy)$(NO_2)_2$(NO)(OH) is shown in Figure 1. All non-hydrogen atoms were refined with anisotropic displace-

(22) Siemens SMART Platform CCD, Siemens Industrial Automation, Inc.: Madison, WI.

(23) An empirical correction for absorption anisotropy: R. Blessing *Acta Crystallogr*. **1995**, *A51*, 33−38.

(24) *SHELXTL-Plus*, V 5.10; Bruker Analytical X-ray Systems: Madison, WI, 1998.

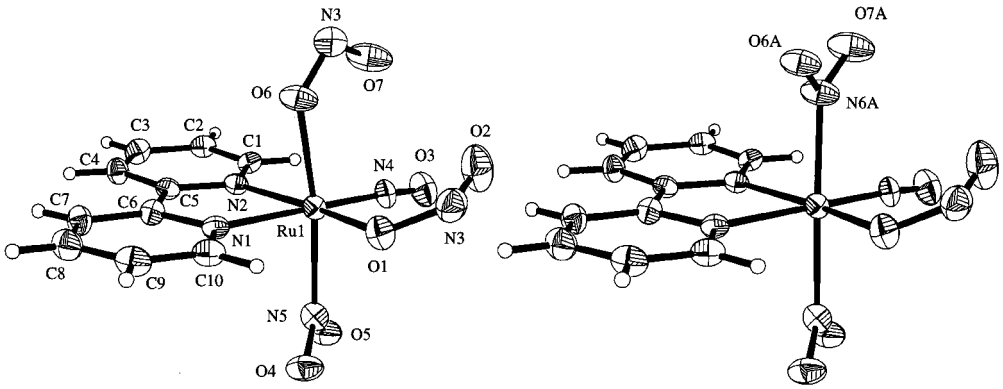

Figure 2. Labeled ORTEP diagram of a solid solution of **2B** and **2C** (30% ellipsoids). All atoms are superimposed except O6, N6, O7 in **2B** and N6A, O6A, O7A in **2C**.

Scheme 1. Reaction Chemistry of $K_2[Ru(bpy)(NO_2)_4]$

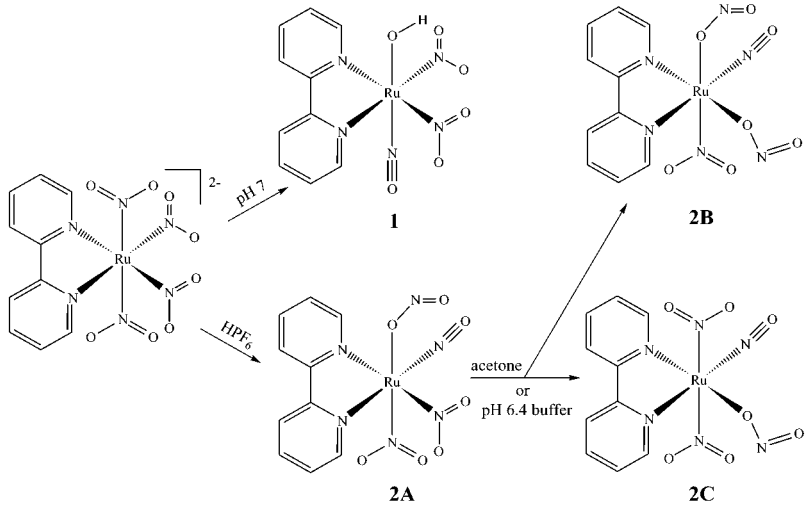

ment parameters. All hydrogen atoms except H9 were located from the electron density map. H9 was restrained as a part of an idealized OH group which was allowed to rotate about the Ru1−O6 bond. All remaining hydrogen atoms were refined in ideal positions with isotropic displacement parameters.

***cis,cis*-Ru(bpy)(ONO)$_2$(NO$_2$)(NO) (2B)/*trans,cis*-Ru(bpy)-(NO$_2$)$_2$(ONO)(NO) (2C) Solid Solution.** A single-crystal suitable for an X-ray structural determination grew from a room-temperature solution of $K_2[Ru(bpy)(NO_2)_4]$ in a 0.1 M pH 6.4 phosphate buffer (see Scheme 1). An ORTEP diagram of **2B**/**2C** is shown in Figure 2. All non-hydrogen atoms were refined with anisotropic displacement parameters. One NO_2^- ligand was modeled as disordered over two sites with different ligation. O6, N6, and O7 form the major nitrito component with 69% occupancy. N6A, O6A, and O7A form the minor nitro component with 31% occupancy. No restraints on bond distances or angles were made in refining the positions of O6, N6, and O7 or N6A, O6A, and O7A. The anisotropic thermal parameters of both the O6, N6, O7 nitrito group and the N6A, O6A, O7A nitro group were restrained to be similar along the directions of the bonds, respectively. The possibility that the disordered NO_2^-/ONO^- ligand is actually a coordinated nitrate was also considered. Attempts to model the electron density in this region with a partially or completely occupied nitrate ligand failed. Spectroscopic evidence also rules out the possibility that this compound contains coordinated nitrate. All hydrogen atoms were refined in ideal positions with isotropic displacement parameters.

Results

Synthesis. Two different compounds were obtained when $[Ru(bpy)(NO_2)_4]^{2-}$ reacted in aqueous solution at different pH values as shown in Scheme 1. Compound **1** is obtained over several days as a pale yellow precipitate if $K_2[Ru(bpy)(NO_2)_4]$ is stirred in a pH 7 buffer. The combustion analysis, NMR, IR, and X-ray crystallography data are all consistent with the formulation of this compound as *cis,trans*-Ru(bpy)-(NO$_2$)$_2$(NO)(OH). The peach-colored compound (**2A**) results from the addition of HPF_6 to an aqueous solution of $K_2[Ru(bpy)(NO_2)_4]$. The combustion analysis, NMR, and IR data are all consistent with the formulation of this material as *cis,cis*-Ru(bpy)(NO$_2$)$_2$(ONO)(NO), where a nitro group *trans* to bpy has been converted to a nitrosyl. Of the three remaining nitro groups, one *cis* to bpy has undergone a linkage isomerization to give the nitrito (Ru−ONO) isomer.

NMR Studies of 1 and 2A. Both compounds were characterized by ^1H and ^{15}N NMR spectroscopy. An ^{15}N NMR spectrum of the parent complex, $K_2[Ru(bpy)(^{15}NO_2)_4]$, (Figure 3A) was acquired for comparison with the new complexes in this study. As expected, two signals are observed for the nitro groups *cis* and *trans* to the bpy. The low solubility of ^{15}N-**1** and ^{15}N-**2A** necessitated the use of a 10 mm bore probe to facilitate the timely acquisition of ^{15}N NMR spectra.

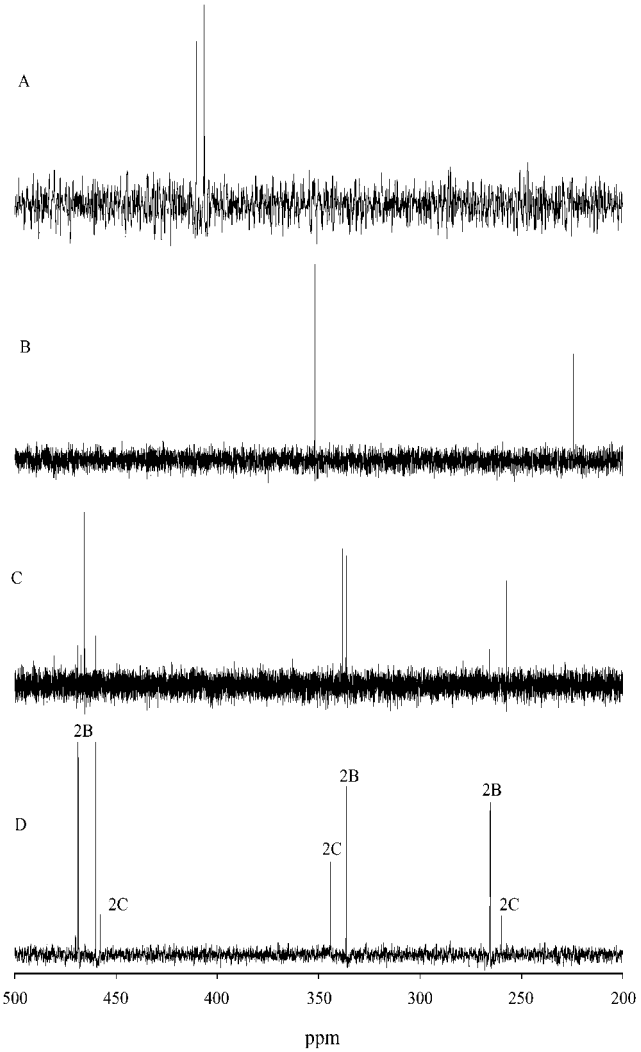

Figure 3. A. ^{15}N NMR (30.45 MHz, D_2O) of $K_2[Ru(bpy)(^{15}NO_2)_4]$. B. ^{15}N NMR (50.67 MHz, D_2O) of **^{15}N-1**. C. ^{15}N NMR (50.67 MHz, d_6-acetone) of **^{15}N-2A**. D. ^{15}N NMR (30.45 MHz, d_6-acetone) of **^{15}N-2B** and **^{15}N-2C** formed from a solution of **^{15}N-2A** after 48 h at room temperature.

The ^{1}H NMR of **1** shows only four resonances, consistent with the presence of identical ligands *trans* to both rings of the bipyridine ligand. None of the bipyridine resonances have chemical shifts greater than 9 ppm, consistent with the nitrosyl ligand occupying an axial site. The ^{15}N NMR spectrum of ^{15}N-**1** is shown in Figure 3B. The ^{15}N NMR shows only two resonances (225 and 352 ppm) with the integration of the latter peak approximately twice that of the former. Comparison with literature data[10] indicates that the peak at 225 ppm can be assigned to a nitrosyl ligand and the peak at 352 ppm is assigned to a nitro ligand. This spectrum is consistent with the presence of two nitro ligands *trans* to each bipyridine ring and one nitrosyl ligand *cis* to bipyridine in the axial position.

The ^{1}H NMR spectrum of **2A** displays eight resonances for the bipyridine protons indicating that different groups occupy the two sites *trans* to bipyridine. A notable feature of this spectrum is the resonance at 9.86 ppm. This is an unusual downfield chemical shift for a bipyridine proton, and it is assigned to H^6 of the bipyridine ring *cis* to a nitrosyl ligand. The unusual downfield shift is due to the position of H^6 in the deshielding region of the anisotropic ring currents of the nitrosyl ligand. The ^{15}N NMR spectrum of ^{15}N-**2A** (Figure 3C) was acquired for a sample of *cis*,*cis*-Ru(bpy)-$(^{15}NO_2)_2(O^{15}NO)(^{15}NO)$ prepared from $K_2[Ru(bpy)(^{15}NO_2)_4]$. The ^{15}N NMR spectrum of ^{15}N-**2A** shows one upfield peak at 257 ppm, two nearly equivalent peaks at 338 and 336 ppm, and a single downfield peak at 466 ppm. Comparison with literature data indicates that the upfield peak can be assigned to a nitrosyl ligand, the peaks at ca. 330 ppm can be assigned to nitro ligands, and the downfield peak can be assigned to a nitrito ligand.[25] The possibility that any of these resonances are due to coordinated nitrate ligands that may have formed because of oxidation by adventitious oxygen is untenable. The chemical shift range of coordinated nitrate (262 ppm (free nitrate) to 237 ppm vs formamide) overlaps only the nitrosyl region of our spectra, but even so, the crystallography and IR spectra are consistent with the presence of nitrosyl ligands not nitrate.[26]

Infrared Spectroscopy of 1 and 2A. The nitrosyl, nitro, and nitrito ligands all have characteristic IR bands that have been discussed previously.[27] Metal−nitro complexes typically exhibit three infrared bands: symmetric (ν_s) and asymmetric stretching modes (ν_{as}) and a bending mode (δ). Metal−nitrito complexes display ν_{N-O} and $\nu_{N=O}$ stretches and an ONO bending mode. Metal−nitrosyl complexes display several bands, the most important of which is the intense ν_{NO} stretch. Metal−hydroxo complexes also display infrared absorptions for the hydroxo ligand stretches.

The IR spectra of **1** and ^{15}N-**1** were collected and compared. Compound **1** has an intense absorption at 1852 cm^{-1} assigned to the ν_{NO} stretch. ^{15}N -**1** shows an isotope shifted ν_{NO} stretch at 1822 cm^{-1}. The observed isotopic shift for the nitrosyl stretch (ratio of energies: $(\nu^{14}_N/\nu^{15}_N = 1.016)$) is very similar to the value obtained using the simple Hooke's law approximation ($\nu^{14}N/\nu^{15}N = 1.018$). Similar NO^+ stretching frequencies are observed for other Ru(II) complexes with a nitrosyl *trans* to a hydroxide. For instance, *trans*-$[Ru(NO)(NH_3)_4(OH)]Cl_2$[28] and *trans*-$[Ru(NO)(OH)(py)_4]^{2+}$ [29] exhibit NO^+ stretches at 1834 and 1868 cm^{-1}, respectively. Peaks that are assigned to the nitro ligands are also observed in the IR spectrum of **1**. The single peak at 1416 cm^{-1} and the two peaks at 1329 and 1309 cm^{-1} can be assigned to the asymmetric and symmetric nitro stretching modes, respectively. ^{15}N-**1** displays the analogous asymmetric and symmetric nitro stretching modes shifted to 1387 cm^{-1} and 1307 and 1291 cm^{-1}, respectively. Two sharp peaks in the spectrum of **1** are observed at 821 and 815 cm^{-1} that can be assigned to the nitro bending motions. These nitro bending motions are shifted about 6 cm^{-1} to lower energy and are split into a total of four bands in the complex ^{15}N-**1**.

(25) Hubbard, J. L.; Zoch, C. R.; Elcesser, W. L. *Inorg. Chem.* **1993**, *32*, 3333.
(26) Mason, J. *Chem. Rev.* **1981**, *81*, 205.
(27) Cotton, F. A.; Wilkinson, G. *Advanced Inorganic Chemistry*, 5th ed.; Wiley: New York, 1988; p 486.
(28) Mercer, E. E.; McAllister, W. A.; Durig, J. R. *Inorg. Chem.* **1966**, *5*, 1881.
(29) Nagao, N.; Hirotaka, N.; Nishimura, H.; Kuroda, H.; Satoh, K.; Howell, F. S.; Mukaida, M. *Bull. Chem. Soc. Jpn.* **1993**, *66*, 1397.

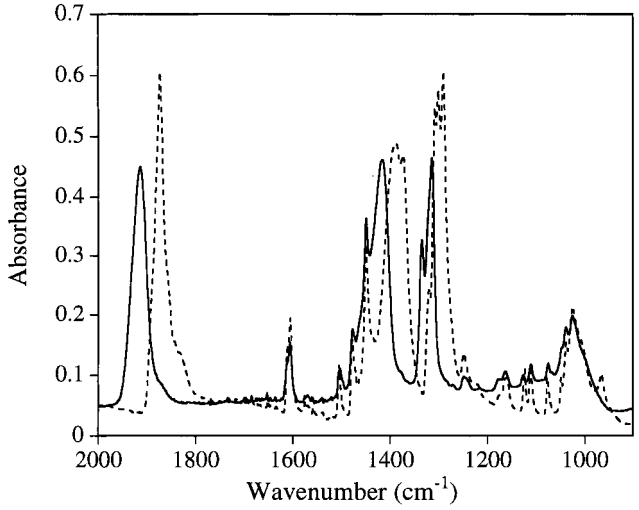

Figure 4. ATR-IR spectra of *cis,cis*-Ru(bpy)$(NO_2)_2$(NO)(ONO) (**2A**) (solid line) and ^{15}N-**2A** (dashed line).

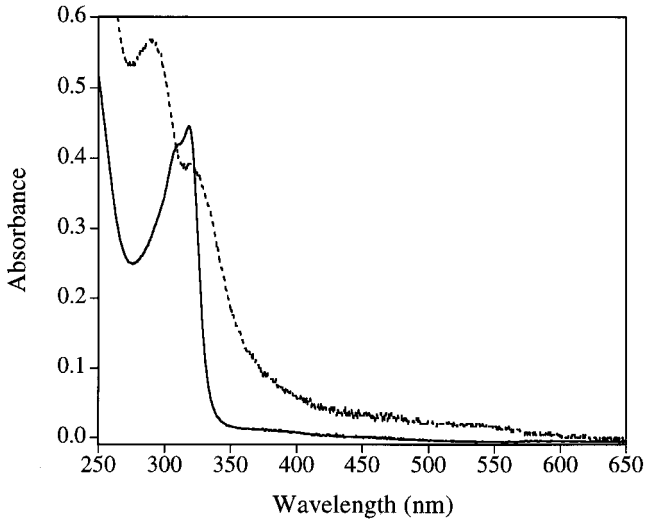

Figure 5. UV−vis spectra of **1** (solid line) in pH 7 buffer and **2A** (dashed line) in pH 4 buffer. The concentration of **1** is 4.3×10^{-5} M, and **2A** is in a saturated solution.

The infrared absorption of **1** at 3495 cm^{-1} is assigned to the O−H hydroxyl stretching mode. The complex *cis,trans*-Ru(dps)$(NO_2)_2$(NO)(OH) (dps = *N,N*′-2,2′-dipyridyl sulfide) exhibits a similar hydroxyl infrared absorbance at 3529 cm^{-1}.[30] The IR spectral bands for the NO^+, NO_2^-, and OH^- ligands are in all regards consistent with the values reported for similar compounds.

The IR spectra of **2A** and ^{15}N-**2A** are shown in Figure 4. The peak at 1914 cm^{-1} is typical for the ν_{NO} stretch for a Ru(II)−NO complex, although it is at the high end of the range for an NO^+ ligand. The labeled complex, ^{15}N-**2A**, displays a nitrosyl stretching mode at 1873 cm^{-1}, and this magnitude of isomer shift is also typical for Ru−NO complexes.[31−33] The experimental $\nu_{^{14}NO}/\nu_{^{15}NO}$ ratio is 1.022, similar to the theoretical value of 1.018 calculated with the Hooke's law approximation. The peak at 1416 cm^{-1} in the spectrum of **2A** shifts ca. 30 cm^{-1} to lower energy, splits into several peaks in the spectrum of ^{15}N-**2A**, and is assigned to the ν_{asym} (NO_2) stretches. The low symmetry of **2A** indicates that all nitro stretches should be active, so the 1416 cm^{-1} band probably represents several coincidentally degenerate bands. The two peaks at 1335 and 1314 cm^{-1} in the spectrum of **2A** also shift approximately 30 cm^{-1} to lower energy in the spectrum of ^{15}N-**2A** and split into a total of 4 peaks. These are assigned to the ν_{sym} (NO_2) stretches. The ca. −30 cm^{-1} shifts for the nitro stretches upon substitution of ^{15}N for ^{14}N is consistent with previously reported data for ruthenium−nitro complexes.[34] Although the ^{15}N NMR of **2A** clearly indicates the presence of a nitrito ligand, less evidence for its presence is found in the IR spectrum. A nitrito ligand typically exhibits ONO stretches at ca.1450 and 1000 cm^{-1}, but the higher energy stretch is often obscured by the presence of NO_2 stretches. In the spectrum of ^{15}N-**2A**, a weak peak is observed at 966 cm^{-1} which is not present in the spectrum of **2A**. This could be the N−O stretch of the nitrito ligand which is obscured by bipyridine peaks in the spectrum of **2A**. Weak, but sharp, bands are also observed in the spectrum of **2A** at 823 and 818 cm^{-1} that shift to 815 and 810 cm^{-1} in the spectrum of ^{15}N-**2A**. These peaks are assigned to the δ_{NO_2} bending motion for the nitro ligands. Again, the IR spectra are consistent with the formulation of **2A** presented here.

UV−Vis Spectra of 1 and 2A. The UV−vis spectra of isolated **1** and **2A** in buffered solutions at pH 7.0 (HEPES) and at pH 4.0 (acetic acid/acetate), respectively, are shown in Figure 5. The absorption bands expected for nitrosyl complexes **1** and **2A** are blue shifted dπ(Ru) → π*(bpy) charge-transfer transitions, intraligand bands associated with the bipyridine ligand, dπ(Ru) → π*(NO^+) charge-transfer transitions, and metal-centered transitions. For both **1** and **2A**, the longer wavelength band in the spectrum of $[Ru(bpy)(NO_2)_4]^{2-}$, previously assigned to an intense dπ(Ru) → π*(bpy) MLCT transition, and a second band at 285 nm (also a dπ(Ru) → π*(bpy) MLCT transition) disappear because the strongly electron withdrawing nitrosyl ligand shifts the charge-transfer bands to higher energy. The intense band present at 320 nm in both complexes **1** and **2A** can be assigned to a bipyridine $\pi \rightarrow \pi^*$ transition. This assignment is consistent with the similar position of this band in both nitrosyl complexes as well as in the $[Ru(bpy)(NO_2)_4]^{2-}$ anion and other related complexes.[1,35,36] The assignment of the 300 nm band in the spectrum of **2A** is less clear. The dπ(Ru) → π*(NO^+) charge transfer bands previously reported in related complexes are usually weak[37−40] ($\epsilon < 50$ M^{-1} cm^{-1}), so these bands, if present, would most likely be obscured. An

(30) Bruno, G.; Nicolo, F.; Tresoldi, G. *Acta Crystallogr., Sect. C* **2000**, *56*, 282.
(31) Leising, R. A.; Kubow, S. A.; Szczepura, L. F.; Takeuchi, K. J. *Inorg. Chim. Acta* **1996**, *245*, 167.
(32) Togano, T.; Kuroda, H.; Nagao, N.; Maekawa, Y.; Nishimura, H.; Howell, F. S.; Mukaida, M. *Inorg. Chim. Acta* **1992**, *196*, 57.
(33) Leising, R. A.; Takeuchi, K. J. *J. Am. Chem. Soc.* **1988**, *110*, 4079.
(34) Leising, R. A.; Kubow, S. A.; Churchill, M. R.; Buttrey, L. A.; Ziller, J. W.; Takeuchi, K. J. *Inorg. Chem.* **1990**, *29*, 1306.
(35) Crosby, G. A. *Acc. Chem. Res.* **1975**, *8*, 231.
(36) Balzani, V.; Boletta, E.; Gandolfi, M. T.; Maestri, M. *Top. Curr. Chem.* **1978**, *75*, 1.
(37) Pell, S.; Armor, J. N. *Inorg. Chem.* **1973**, *12*, 873.

attractive possibility is that the 300 nm band represents a blue shifted dπ(Ru) → π*(bpy) charge-transfer transition.

Isomerization of 2A. Significant changes are observed in the ^{1}H and ^{15}N spectra if a d_6-acetone solution of **2A** is allowed to sit for several days at room temperature. The same products are also observed to form in D_2O and CH_2Cl_2 solutions of **2A**. Although the ^{1}H NMR spectrum of the products is complicated, the presence of two doublets near 10 ppm suggests that there are two new products and each has a nitrosyl ligand *cis* to the bipyridine ring. Each product has eight bipyridine resonances, indicating that different ligands occupy the sites *trans* to bipyridine. The ^{15}N NMR spectrum of this solution (Figure 3D) also shows two products. The peaks are assigned to the same two products observed by ^{1}H NMR and are labeled **2B** and **2C** in Figure 3D. Product **2B** is dominant and displays two downfield peaks at 469 and 460 ppm and single peaks at 337 and 266 ppm. The minor product (**2C**) displays single peaks at 458, 344, and 260 ppm with the integration of the resonance at 344 ppm clearly greater than the other two.

X-ray Studies of 1 and 2B/2C. Single-crystal X-ray data were obtained for **1**. The ORTEP is shown in Figure 1, and selected bond lengths and angles are given in Table 2. The structure shows the complex has N-bound nitro groups *trans* to both rings of the bipyridine ligand with nitrosyl and hydroxo groups occupying the remaining sites *cis* to bipyridine. Although the hydroxyl proton was not located in the electron density map, the spectroscopic (observed ν_{OH}) and crystallographic evidence are consistent with O6 as a part of a Ru(II)−OH group. The counterions required for either a Ru(II)−oxo or Ru(II)−(OH_2) formulation of this complex were not observed, and the bond distance for Ru(1)−O(6) (1.917(2) Å) is also more reasonable for Ru(II)−OH than for either Ru(II)−oxo or Ru(II)−(OH_2). A search of the Cambridge Structural Database reveals several examples of a Ru(II)(bpy)(OH_2)$^{n+}$ moiety with an average Ru−OH_2 bond distance of 2.124 Å[41] and no examples of Ru(II)−oxo complexes. The geometry around the ruthenium is essentially octahedral with some distortion due to the bite angle of the bpy ligand (N(1)−Ru−N(2) angle of 78.66(10)°). The angles between the bpy nitrogens and the *cis* nitro groups are correspondingly greater than 90° (96.69(10)° and 96.91(10)°). All other angles between *cis* ligands are very close to 90°. The two nitro groups are both rotated to approximately the same angle but in opposite directions from the plane of symmetry which bisects the bipyridine ligand. The torsion angles are 29.7(3)° for O(6)−Ru(1)−N(4)−O(3) and 23.8(3)° for O(6)−Ru(1)−N(3)−O(2). The oxygen atoms O2 and O3 of the nitro groups are within hydrogen bonding distances of the hydroxyl group hydrogen (H(6A)−O(2) 2.39 Å, H(6A)−O(3) 2.42 Å). The Ru(1)−N(3) and Ru(1)−N(4) bond lengths are essentially identical at 2.081(3) and 2.076(2) Å, respectively. The nitrosyl group is close to linear with a O(5)−N(5)−Ru(1) angle of 174.5(3)°. As has been previously observed for complexes with a π-donor *trans* to a nitrosyl ligand, the Ru−NO bond is longer than typically observed while the Ru−OH bond is shorter than typically observed.[42−44]

The X-ray structure determination of **2B/2C** reveals evidence for a solid solution of linkage isomers of **2A** *cis*,*cis*-Ru(bpy)(NO_2)$_2$(ONO)(NO). The ORTEP diagrams are shown in Figure 2, and selected bond lengths and angles are given in Table 2. The structure shows both linkage isomers have an O-bound nitrito group, a nitrosyl ligand *trans* to bipyridine, and an N-bound nitro group occupying a site *cis* to the bipyridine. The remaining ligand in the other axial position was modeled as disorder between the two linkage isomers; the major component is a nitrito ligand (O6, N6, O7) with an occupancy of 69% while the minor component is a nitro ligand (N6A, O6A, O7A) with an occupancy of 31%. This crystal structure is consistent with a solid solution of **2B** and **2C**. The angle between the least-squares planes formed by Ru(1)−N(6)−O(6)−O(7) and Ru(1)−N(6A)−O(6A)−O(7A) is 14.6°. The geometry about Ru(1) is effectively octahedral with distortions from the bite angle of bipyridine (N(1)−Ru−N(2) angle of 77.78(18)°) and the O-bound nitrito ligands. The angles between ligands *trans* to nitro (N(5)−Ru(1)−N(6A) of 177.1(8)°) and nitrosyl ligands (N(4)−Ru(1)−N(2) of 172.5(2)°) are closer to 180° than for nitrito ligands (N(5)−Ru(1)−O(6) of 167.9(3)° and O(1)−Ru(1)−N(1) of 166.92(18)°). The nitrosyl ligand is almost linear with an O(3)−N(4)−Ru(1) angle of 172.5(5)°. A search of the Cambridge Structural Database reveals that this structure is the only crystallographically characterized example of a ruthenium complex with nitrosyl, nitro, and nitrito ligands.

Kinetic Studies of the Formation of 1 and 2A in Aqueous Solutions. The reactions of K_2[Ru(bpy)(NO_2)$_4$] in buffered solutions were studied at eight different pH values between 2.9 and 9.0 to determine the rate laws. The representative changes observed in the UV−vis spectrum of K_2[Ru(bpy)(NO_2)$_4$] in buffered solutions at pH 7.0 (HEPES) are shown in Figure 6. Analogous changes that occur at pH 4.0 (acetic acid/acetate) are shown in the Supporting Information. The final spectrum at pH 7.0 is identical to the UV−vis spectrum of a bulk sample of **1** in the same buffer. In all cases, isosbestic points are maintained, indicating that the conversion of the starting material to product occurs

(38) Schreiner, A. F.; Lin, S. W.; Hauser, P. J.; Hopcus, E. A.; Hamm, D. J.; Gunter, J. D. *Inorg. Chem.* **1972**, *11*, 880.
(39) Lebrero, M. C. G.; Scherlis, D. A.; Estiu, G.; Olabe, J. A.; Estrin, D. A. *Inorg. Chem.* **2001**, *40*, 4127.
(40) Manoharan, P. T.; Gray, H. B. *J. Am. Chem. Soc.* **1965**, *87*, 3340.
(41) (a) Cheng, W.-C.; Yu, W.-Y.; Cheung, K.-K.; Che, C.-M. *J. Chem. Soc., Dalton Trans.* **1994**, 57. (b) Reddy, K. B.; Cho, M.-O. P.; Wishart, J. F.; Emge, T. J.; Isied, S. S. *Inorg. Chem.* **1996**, *35*, 7241. (c) Weathers, N. R.; Sadoski, R. C.; Durham, B.; Cordes, A. W. *Acta Crystallogr., Sect. C* **1997**, *53*, 1047. (d) Homanen, P.; Haukka, M.; Ahlgren, M.; Pakkanen, T. A. *Inorg. Chem.* **1997**, *36*, 3794. (e) Cheng, W.-C.; Yu, W.-Y.; Zhu, J.; Cheung, K.-K.; Peng, S. M.; Poon, C.-K.; Che, C.-M. *Inorg. Chim. Acta* **1996**, *242*, 105. (f) Cheung, K. K.; Peng, S. M.; Poon, C. K.; Che, C.-M. *Inorg. Chim. Acta* **1996**, *242*, 105. (g) Fung, W.-H.; Cheng, W.-C.; Yu, W.-Y.; Che, C.-M.; Mak, T. C. W. *Chem. Commun.* **1995**, 2007.
(42) Nishimura, H.; Matsuzawa, H.; Togano, T.; Mukaida, M.; Kakihano, H.; Bottomley, F. *J. Chem. Soc., Dalton Trans.* **1990**, 137.
(43) Blake, A. J.; Gould, R. O.; Johnson, B. F. G.; Parisini, E. *Acta Crystallogr., Sect. C* **1992**, *C48*, 982.
(44) Gromilov, S. A.; Alekseev, V. I.; Emelyanov, V. A.; Baidina, I. A. *Acta Crystallogr., Sect. C*. **1996**, *C52*, 288.

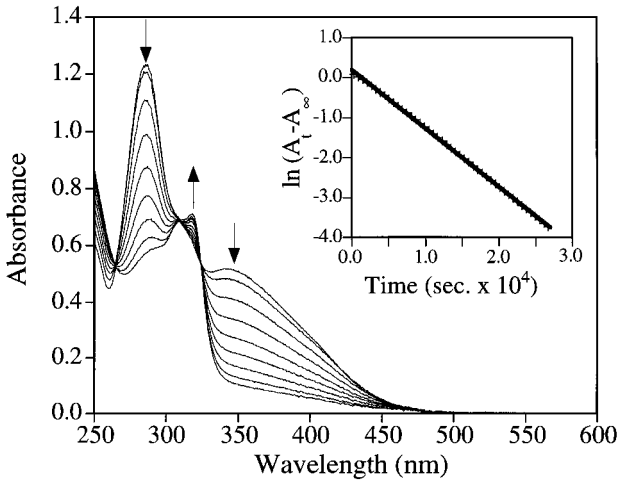

Figure 6. UV−vis spectral changes during the reaction of $[Ru(bpy)(NO_2)_4]^{2-}$ in a pH 7.0 buffer. Arrows show the change in direction with time. Inset shows a representative pseudo-first-order kinetic plot for the change in absorbance at 400 nm.

Table 3. Kinetic Data[a] for the Decomposition of $[Ru(bpy)(NO_2)_4]^{2-}$ as a Function of pH

pH[b]	k_{obs} (s^{-1})[c]
2.90	0.021
3.00	0.017
3.28	0.0094
3.51	0.0060
4.00	0.0023
5.00	3.2×10^{-4}
7.00	1.4×10^{-4}
8.98	1.6×10^{-4}

[a] Data were recorded at 25 ± 0.5 °C. [b] See Experimental Section for details. [c] k_{obs} is the observed rate constant. Values are an average of three determinations except for the value at pH 8.98 which is an average of two. Error in k_{obs} values average ±5%.

without the buildup of significant concentrations of intermediate species or the formation of secondary products; additionally, all plots of $\ln(A_t - A_\infty)$ versus t are linear for at least four half-lifes. The observed pseudo-first-order rate constants (k_{obs}) obtained at each pH are given in Table 3. A plot of k_{obs} versus pH is shown in Figure 7. The line drawn through the data is the calculated fit to eq 3 with $a = 1.5(1) \times 10^{-4}$ s^{-1} and $b = 18(0.8)$ s^{-1} M^{-1}.

$$k_{obs} = a + b[H^+] \quad (3)$$

Discussion

The products obtained from the reaction of $[Ru(bpy)(NO_2)_4]^{2-}$ in aqueous solution are pH dependent. As expected from previous studies, both products contain nitrosyl groups formed from the deoxygenation of a nitro group. The nitrosyl stretching frequencies in the infrared spectra of both components are consistent with the formal assignment of the nitrosyl ligands as NO^+. We were able to assign the structures of **1** and **2A** from ^1H and ^{15}N NMR spectral data. For **1**, the ^1H NMR spectrum clearly shows a symmetrical bipyridine ligand with identical ligands in the *trans* positions. The ^{15}N NMR spectrum shows only two peaks for **1** which can be assigned by their chemical shifts to N-bound nitro and nitrosyl groups. The ^{15}N NMR spectrum suggests that **1** could

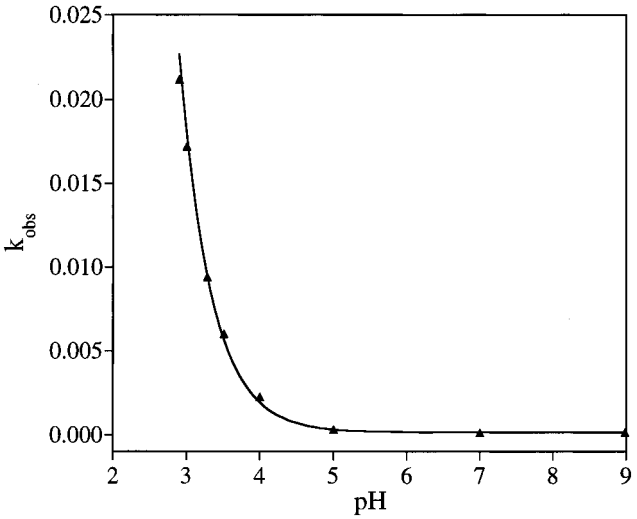

Figure 7. Plot of k_{obs} vs pH for the reaction of $[Ru(bpy)(NO_2)_4]^{2-}$. The multivariable best fit line is based on eq 3 with fitting parameters $a = 1.5(1) \times 10^{-4}$ s^{-1} and $b = 18(0.8)$ s^{-1} M^{-1}.

be either *cis*,*trans*-$Ru(bpy)(NO)_2(NO_2)(OH)$ or *cis*,*trans*-$Ru(bpy)(NO_2)_2(NO)(OH)$. The former complex should exhibit two nitrosyl bands in the IR. The presence of a single nitrosyl stretch in the IR indicates the two identical ligands *trans* to bipyridine must be nitro ligands with the nitrosyl ligand in the axial position. The ligand *trans* to the nitrosyl can be inferred to be a hydroxyl group from the low frequency of the nitrosyl stretch in the IR, the O−H stretch of the hydroxyl group, and X-ray crystallographic evidence.

The ^1H NMR spectrum of **2A** is dramatically different, showing eight resonances for the bipyridine indicating that the metal is asymmetrically substituted in the *trans* positions. We conclude that one of the *trans* ligands is a nitrosyl on the basis of the presence of the bpy ^1H NMR signal shifted to almost 10 ppm. Although the ^1H NMR suggests that **2A** is *mer*-$Ru(bpy)(NO_2)_3(NO)$, the ^{15}N NMR shows *four* resonances that are assigned by chemical shift to one nitrosyl ligand, two inequivalent nitro ligands, and a nitrito ligand. If one of the sites *trans* to bpy is occupied by a nitrosyl ligand, the two nonequivalent nitro ligands must occupy different positions relative to bpy, one *trans* to bpy and one *cis*, leaving the final position *cis* to bpy to be occupied by the nitrito ligand, giving the structure shown in Scheme 1.

With the assignment of the structures of **1** and **2A** firmly in hand, we turn our attention to the chemistry of their formation. There are many kinetic studies of the M−nitro → M−nitrosyl conversion, but only a few for M = Ru(II),[45] and only one study[46] of the reverse reaction (such as occurs in the formation of **1** and **2A**) with M = Ru(II). With this in mind, we examined the reaction kinetics of $K_2[Ru(bpy)(NO_2)_4]$ in buffered aqueous solutions. Our kinetic data clearly show the formation of **1** and **2A** are first order in $[Ru(bpy)(NO_2)_4]^{2-}$ from pH 2.90 to pH 8.98. The dependence

(45) (a) Mondal, B.; Paul, H.; Puranik, V. G.; Lahiri, G. K. *J. Chem. Soc., Dalton Trans.* **2001**, *4*, 481−487. (b) Chevalier, A. A.; Gentil, L. A.; Olabe, J. A. *J. Chem. Soc., Dalton Trans.* **1991**, *8*, 1959−63.
(46) Bowden, W. L.; Little, W. F.; Meyer, T. J. *J. Am. Chem. Soc.* **1976**, *98*, 444.

on the H^+ concentration is more complex. The excellent fit of the data (Figure 7) to eq 3 indicates that the formation of **1** and **2A** occurs by two competing mechanisms. At high pH (>6), **1** is formed by a pH independent mechanism with a first-order rate constant of $1.5(1) \times 10^{-4}$ s^{-1}. The second pathway that produces **2A** is first order in the concentration of H^+ and becomes important at lower pH. The apparent rate constant for this pathway is 18 M^{-1} s^{-1}. These data are consistent with the synthetic chemistry; although **1** is also formed at low pH in the synthetic reactions, **2A** is the predominant product.

We propose mechanisms for the formation of **1** and **2A** that are consistent with these data. For the formation of **2A**, the simplest possibility is the protonation of $[Ru(bpy)(NO_2)_4]^{2-}$ in an irreversible bimolecular step (reaction 4) that is rate determining:

$$[Ru(bpy)(NO_2)_4]^{2-} + H^+ \rightarrow [Ru(bpy)(NO_2)_3(HNO_2)]^+ \quad (4)$$

In subsequent rapid steps, hydroxide is lost to form the nitrosyl ligand, and a nitro ligand isomerizes to a nitrito ligand. The rate law for this mechanism is shown in eq 5.

$$\text{rate} = k[[Ru(bpy)(NO_2)_4]^{2-}][H^+] \quad (5)$$

This mechanism is untenable for several reasons. First, the protonation step should be very rapid in the forward direction and reversible.[47] Second, it is not reasonable for the formation of the nitrosyl and the linkage isomerization reactions to both be faster than a simple protonation step.

A second, more reasonable possibility is a rapid preequilibrium involving the reversible protonation of a nitro group followed by loss of hydroxide to give $Ru(bpy)(NO_2)_3(NO)$ as an intermediate in the rate-determining step (reactions 6 and 7). This mechanism has been previously proposed to describe the conversion of $[Fe(CN)_5NO_2]^{4-}$ to $[Fe(CN)_5NO]^{2-}$ in the pH range from 4 to 11.[46]

$$[Ru(bpy)(NO_2)_4]^{2-} + H^+ \underset{k_{-1}}{\overset{k_1}{\rightleftharpoons}} [Ru(bpy)(NO_2)_3(HNO_2)]^- \text{ (fast)} \quad (6)$$

$$[Ru(bpy)(NO_2)_3(HNO_2)]^- \xrightarrow{k_2} Ru(bpy)(NO_2)_3(NO) + OH^- \text{ (slow)} \quad (7)$$

$$Ru(bpy)(NO_2)_3(NO) \xrightarrow{k} \mathbf{2A} \text{ (fast)} \quad (8)$$

The rate law for this mechanism is given in eq 9.

$$\text{rate} = \frac{k_2K_1[H^+]}{1 + K_1[H^+]}[[Ru(bpy)(NO_2)_4]^{2-}] \quad (9)$$

In buffered solutions, this rate law gives a k_{obs} that will show saturation behavior when $K_1[H^+] \gg 1$. Even for data at the lowest pH used, our kinetic data do not show this saturation effect, so $K_1[H^+] \ll 1$, and the k_{obs} is an apparent second-order rate constant with the value of $k_2K_1 = 18$ M^{-1} s^{-1}. Realizing that K_1 is $1/K_a$ for the protonated form of the coordinated nitro group and saturation behavior described by eq 9 commences when the pH approaches the pK_a, we estimate that the pK_a value for protonated $[Ru(bpy)(NO_2)_4]^{2-}$ is no greater than 2. This pK_a value is smaller than the value measured for $[Fe(CN)_5NO_2H]^{3-}$ (pK_a = 6.4) but in line with the decrease in negative charge on the $[Ru(bpy)(NO_2)_4]^{2-}$ anion, and with the presence of stronger π acid ligands. Using a value of 2 for the pK_a of protonated $[Ru(bpy)(NO_2)_4]^{2-}$, k_2 is estimated to be 0.18 s^{-1}. This value is much smaller than the 500 s^{-1} measured for the $[Fe(CN)_5NO_2]^{4-}$ to $[Fe(CN)_5NO]^{2-}$ conversion[46] and is consistent with the electron defficient nature of $[Ru(bpy)(NO_2)_4]^{2-}$ relative to $[Fe(CN)_5NO_2]$.$^{4-}$ To be internally consistent, this analysis also requires the rate constant for the nitro−nitrito linkage isomerization in eq 8 that follows the rate determining step to be faster than k_2. Although Ru(II) nitro to nitrito isomerization reactions can be slow,[48] there is an example of one complex with π acceptor ligands that is fast,[47] which is consistent with Ru(III) nitro to nitrito isomerizations which are usually fast.[13,27,49−52] The sequence of steps shown in eqs 6−8 is also consistent with Ru−nitrosyl → Ru−nitro conversions previously studied. These studies show hydroxide attack at nitrosyl (the reverse of the rate determining step 7) as rate determining.

Although compound **1** also contains a nitrosyl ligand, the lack of pH dependence in the rate law for its formation suggests a rate determining step quite different from that required to form **2A**. As many nitro complexes are stable toward deoxygenation at high pH (pH > ca. 6), a prior ligand substitution that promotes nitrosyl formation is more reasonable. For example, the equilibrium constants for the nitro/nitrosyl interconversion of $[Ru(bpy)(trpy)(NO_2)]^+$ and $[Ru(bpy)_2(py)(NO_2)]^+$ show that the approximate pH values at which equal amounts of the nitro and nitrosyl complexes are present are 2.3 and 4.0, respectively.[53] We expect that the deoxygenation equilibrium constant for $[Ru(bpy)(NO_2)_4]^{2-}$ should be comparable to these complexes on the basis of the similar angular overlap parameter (e_π) for the two types of ligands ($e_\pi(NO_2^-) = -1160$ cm^{-1}; $e_\pi(bpy) = -1600$ cm^{-1})[54] involved. If anything, the slightly less negative e_π value for the nitro ligand should stabilize the nitro form of the tetranitro complex relative to the polypyridyl complexes.

A plausible rate-limiting step for the formation of **1** is substitution of a nitro group in $[Ru(bpy)(NO_2)_4]^{2-}$ by water. We have observed that one nitro group of $[Ru(bpy)(NO_2)_4]^{2-}$ can be readily replaced by pyridine at room temperature to produce *fac*-$[Ru(bpy)(NO_2)_3(py)]^{-1}$.[1] A similar reaction with

(47) Masek, J.; Wendt, H. *Inorg. Chim. Acta* **1969**, *3*, 455.
(48) Ooyama, D.; Nagao, N.; Nagao, H.; Miura, Y.; Hasegawa, A.; Ando, K.-I.; Howell, F. S.; Mukaida, M.; Tanaka, K. *Inorg. Chem.* **1995**, *34*, 6024.
(49) Keene, F. R.; Salmon, D. J.; Walsh, J. L.; Abruna, H. D.; Meyer, T. J. *Inorg. Chem.* **1980**, *19*, 1896.
(50) Nagao, H.; Nishimura, H.; Kitanaka, Y.; Howell, F. S.; Mukaida, M.; Kakihana, H. *Inorg. Chem.* **1990**, *29*, 1693.
(51) Nagao, H.; Mukaida, M.; Shimizu, K.; Howell, F. S.; Kakihana, H. *Inorg. Chem.* **1986**, *25*, 4312.
(52) Ooyama, D.; Nagao, H.; Nagao, N.; Howell, F. S.; Mukaia, M. *Chem. Lett.* **1996**, 759.
(53) Pipes, D. W.; Meyer, T. J. *Inorg. Chem.* **1984**, *23*, 2466.
(54) Hoggard, P. E.; Clanet, P. P. *Polyhedron* **1987**, *7*, 1621.

water first produces *fac*-$[Ru(bpy)(NO_2)_3(H_2O)]^-$ (reaction 10) in the rate determining step:

$$[Ru(bpy)(NO_2)_4]^{2-} + H_2O \rightarrow \textit{fac}\text{-}[Ru(bpy)(NO_2)_3(H_2O)]^- + NO_2^- \quad (10)$$

A sequence of fast subsequent steps that include the loss of a proton from the coordinated water and deoxygenation of the *trans* nitro group would then form **1**. Regardless of the order of these subsequent steps, the formation of **1** is driven by the complementary nature of the π-acid nitrosyl group and the *trans* π-donor hydroxo group.

The presence of the nitrito ligand in *cis,cis*-$Ru(bpy)(NO_2)_2(NO)(ONO)$ (**2A**) raised the interesting question as to whether other linkage isomers could be obtained via the isomerization of the remaining nitro groups. When a solution of **2A** in acetone was allowed to sit at room temperature for several days, two new products formed in a 4.6:1 ratio. Both products still exhibit resonances in the ^{1}H NMR spectrum consistent with two different ligands *trans* to bpy. The extreme downfield position of one bpy resonance in each new product suggested that they each contain a nitrosyl ligand *trans* to bipyridine. ^{15}N NMR shows the major product has one nitrosyl, one nitro, and two nitrito ligand ^{15}N resonances and is assigned as structure **2B** (shown in Scheme 1) where a second nitro ligand has undergone a linkage isomerization to produce *cis,cis*-$Ru(bpy)(ONO)_2(NO_2)(NO)$. The minor product (**2C**) has one ^{15}N NMR peak in each of the nitrosyl, nitro, and nitrito regions. Two likely candidates for this species are *trans,cis*-$Ru(bpy)(NO_2)_2(NO)(ONO)$ or *trans,cis*-$Ru(bpy)(ONO)_2(NO_2)(NO)$. As the ^{15}N NMR spectrum shows that the integration of the resonance in the nitro region is twice that of the peaks in the nitrosyl and nitrito regions, we assign **2C** as *trans,cis*-$Ru(bpy)(NO_2)_2(NO)(ONO)$. These ^{15}N NMR assignments are consistent with the X-ray structure of the rearrangement products of **2A** in pH 6.4 phosphate buffer. This structure is a solid solution of **2B**/**2C**, the two linkage isomers in a 69:31 ratio with **2B** as the major product and **2C** as the minor product.

Isomer **2B** is likely the predominant isomer because electron deficiency at ruthenium, imparted by the strong π-acceptor ligands nitrosyl, nitro, and bpy, is offset by two nitrito π-donors *trans* to π-acceptors. In **2C**, only one nitrito ligand, *trans* to the π-acceptor bpy, is present to partially alleviate the electron deficiency at ruthenium. A fourth possible isomer, *trans,cis*-$Ru(bpy)(ONO)_2(NO_2)(NO)$, seems least likely to form because this configuration has nitrosyl, nitro, and bpy ligands all in the same plane, leaving the π-donor nitrito ligands only *cis* to the π-acceptor ligands rather than in the more stabilizing *trans* position.

Conclusions

We have observed that two different nitrosyl containing complexes can be prepared from aqueous solutions of $[Ru(bpy)(NO_2)_4]^{2-}$, depending on the pH. At low pH values, *cis,cis*-$Ru(bpy)(NO_2)_2(ONO)(NO)$ (**2A**) is formed directly from the deoxygenation of one nitro group and the subsequent rapid linkage isomerization of a second nitro group. This complex undergoes further thermal linkage isomerization reactions in solution to produce a mixture of *cis,cis*-$Ru(bpy)(ONO)_2(NO_2)(NO)$ (**2B**) and *trans,cis*-$Ru(bpy)(NO_2)_2(ONO)(NO)$ (**2C**) that was characterized by X-ray crystallography. At higher pH values, $[Ru(bpy)(NO_2)_4]^{2-}$ undergoes a pH independent substitution of a nitro ligand by water followed by nitro deoxygenation to produce *cis,trans*-$Ru(bpy)(NO_2)_2(NO)(OH)$ (**1**). The lability of the nitro groups and the facile conversion of a remaining nitro group to nitrosyl suggests that the $[Ru(bpy)(NO_2)_4]^{2-}$ anion may be a potential synthon for a variety of new ruthenium−nitrosyl complexes. Further investigations along these lines are in progress.

Acknowledgment. D.A.F acknowledges the financial support of The State University of New York at New Paltz. K.R.M. acknowledges the financial support of the National Science Foundation, Grant CHE-9307837. Letitia Yao is acknowledged for her contributions to the acquisition of ^{15}N NMR spectra at the University of Minnesota NMR Facility. We also acknowledge the University of Minnesota X-ray Crystallographic Laboratory.

Supporting Information Available: Figure 6B and X-ray crystallographic files in CIF format. This material is available free of charge via the Internet at http://pubs.acs.org.

IC0255205